Electronic Supplementary Material (ESI) for Dalton Transactions.
This journal is © The Royal Society of Chemistry 2017

Supporting information

Mechanistic Study of Nitrite Reduction by Iron(II) Complexes of Methylated N-Confused Porphyrins: Evidence of Porphyrinic Acidic Protons on Reactivities

Wei-Min Ching,[a, c] Peter Ping-Yu Chen,[b] and Chen-Hsiung Hung*[a]

Contents

1. General Information
2. Synthesis of [Fe^{II}(*H*CTPP*Me*)Br] (1), [Fe^{II}(d_{20}-*H*CTPP*Me*)Br] (1a), [Fe^{II}(*H*CTPPCD_3)Br] (1b) and [Fe^{II}(*Me*CTPP*Me*)Br] (2).
3. Synthesis of [Fe(CTPPCH_2)(NO)] (3).
4. Synthesis of [Fe(CTPPCH_2)(^{15}NO)] (3a).
5. Synthesis of [Fe(d_{20}-CTPPCH_2)(NO)] (3b).
6. Synthesis of [Fe(CTPPCD_2)(NO)] (3c).
7. Time-dependent IR spectra of mixing [Fe^{II}(*H*CTPP*Me*)Br] (1) with [KNO_2][18-crown-6 ether].
8. Reaction of [Fe^{II}(*H*CTPP*Me*)Br] (1) with 1 equiv [PPN][NO_2] and hydroquinone.
9. Reaction of [Fe^{II}(*H*CTPP*Me*)Br] (1) with 1 equiv [PPN][NO_2] in THF.
10. Reaction of [Fe^{II}(*Me*CTPP*Me*)Br] (2) with $NaNO_2$.
11. Reaction of [Fe^{II}(*H*CTPP*Me*)Br] (1) with NaOMe than reacting with $NaNO_2$.
12. DFT calculations.
13. X-ray Single crystal structural determination.

Figure S1. IR spectrum of Fe(CTPPCH_2)NO (**3**) and Fe(CTPPCH_2)^{15}NO (**3a**).

Figure S2. ^{1}H-^{13}C-HSQC of Fe(CTPPCH_2)NO (3) and inserted region of the methylene group.

Figure S3. ^{13}C-NMR (upper) and DEP 135 (lower) of Fe(CTPPCH_2)NO (**3**, lower); blue asterisk marks the carbon alongside the outer nitrogen and yellow asterisk marks the carbon of methylene group.

Figure S4. ^{1}H-^{13}C-HMBC of Fe(CTPPCH_2)NO (**3**) and inserted region of the inner-carbon.

Figure S5. ^{15}N-NMR spectrum Fe(CTPPCH_2)^{15}NO **(3a**).

Figure S6. [Fe^{II}(*H*CTPP*Me*)Br] (**1**) reacted with 1 $PPNNO_2$ and hydroquinone in 4 hours.

Figure S7. UV-Vis spectra of [Fe(CTPPCH_3)NO] (**5**, solid line), [Fe(*H*CTPPCH_2)NO][BF_4] (4, dotted line) and [Fe(CTPPCH_2)NO] (3, dashed line).

Figure S8. ESI-Mass spectrum of Reaction of [Fe^{II}(*HCTPPMe*)Br] (**1**) with 1 equiv [PPN][NO_2] in THF.

FigureS9. ESI-Mass spectrum analysis of [Fe^{III}(CTPP*Me*)]$_2$O $[M+H]^+$.

Figure S10. ESI-Mass spectrum analysis of [Fe(CTPP*Me*)(NO_2)] $[M]^+$.

Figure S11. ESI-Mass spectrum analysis of [Fe(CTPP*Me*)(THF)] $[M+H]^+$.

Figure S12. ^{1}H NMR spectrum of Reaction of [Fe^{II}(*HCTPPMe*)Br] (**1**) with 1 equiv [PPN][NO_2] in

THF: Fe(CTPP*Me*)NO (**4**, blue marks), [Fe(CTPP*Me*)]$_2$O (red marks), and Fe(CTPP*CH$_2$*)NO (**3**, orange marks).

Figure S13. UV-Vis spectrum of Fe^{II}(*Me*CTPP*Me*)Br (**2**).

Figure S14. Fe^{II}(*Me*CTPP*Me*)Br (**2**) reacts with 1 equiv $NaNO_2$ for 24 hours.

Figure S15. ^{1}H-NMR spectra of Fe^{II}(*Me*CTPP*Me*)Br (**2**, upper) and reaction after 24 hours (lower).

Figure S16. Cyclic voltammograms of Fe^{II}(*H*CTPP*Me*)Br (**1**) and Fe^{II}(*Me*CTPP*Me*)Br (**2**; vs $FeCp_2$).

Figure S17. Optimized structures of **6a** (a), **6b** (b), **7a** (c), **7b** (d), **8a** (e), **8b** (f), **9a** (g), **9b** (h), **10** (i), **11** (j), **12** (k), **13** (l), **14** (n), and **15** (m).

Table S1. Optimized structures bond distances and Relative energies of Fe^{II}(NCP*Me*)(HNO$_2$) (**6a**).

Table S2. Crystal Data and Structure Refinement for Fe^{II}(*Me*CTPP*Me)*Br **(2)** and Fe(CTPP*CH$_2$*)NO **(3).**

1. General Information. Dichloromethane, *n*-hexane, methanol and THF were degassed and dried under N_2 using PS-400 solvent purification system (Innovative Technology) equipped with activated alumina stainless steel columns. Each freshly distilled solvent was stored in a round-bottom flask with J-Young tap, sent into an inert atmosphere dry box, and bubbled with nitrogen for at least 30 min to remove any residual oxygen. UV-Vis spectrum and its time-course measurements were recorded with an Agilent 8453 spectrophotometer. FT-IR measurements were carried out by a Perkin Elmer Paragon 1000 spectrophotometer. The ESI mass spectrum was recorded on a QSTAR™ Hybrid LC/MS/MS system. ^{1}H NMR spectra were recorded on a Bruker Spectrospin 400 Ultra ShieldTM and a Bruker Spectrospin 500 Ultra ShieldTM spectrometer. ^{15}N NMR spectrum was also carried out by a Bruker Spectrospin 500 Ultra ShieldTM spectrometer. ^{2}H, ^{13}C, HSQC, and HMBC were recorded on a Bruker Spectrospin DRX 500. Cyclic voltammetric measurements were performed using a CHI 600D Potentiostat/Galvanostat (CH Instruments, Inc.). The cell consists of a Pt working electrode, a Pt wire auxiliary electrode, and a silver wire reference electrode, with 0.1 M tetra-*n*-butylammonium hexafluorophosphate ([Bu$_4$N]PF$_6$) as the supporting electrolyte in dichloromethane. Ferrocene was used as external standard for all measurements. The preparations of inner carbon and inner carbon/outer nitrogen double methyl substituted N-confused porphyrins, [(CTPP*Me*)H$_2$], [(d$_{20}$-CTPP*Me*)H$_2$], [(CTPP*CD$_3$*)H$_2$], [(*Me*CTPP*Me*)H], Fe(CTPP*Me*)NO (**5**), and [Fe(CTPP*CH$_2$*)NO][BF$_4$] (**4**) were followed the literature method.[1-4]

2. Synthesis of [Fe^{II}(*H*CTPP*Me*)Br] (1), [Fe^{II}(d$_{20}$-*H*CTPP*Me*)Br] (1a), [Fe^{II}(*H*CTPP*CD$_3$*)Br] (1b) and [Fe^{II}(*Me*CTPP*Me*)Br] (2). The iron(II) N-Confused porphyrin complexes, [Fe^{II}(*H*CTPP*Me*)Br] (1), [Fe^{II}(d$_{20}$-*H*CTPP*Me*)Br] (**1a**), [Fe^{II}(*H*CTPP*CD$_3$*)Br] (**1b**) and [Fe^{II}(*Me*CTPP*Me*)Br] (2), were prepared using methods modified from literature procedures.[5-7] Reactions of the single and double methyl substituted N-confused porphyrin ligands with $FeBr_2$ in the basic conditions under an inert-atmosphere dry box resulted in the iron complexes (**1**), (**1a**), (**1b**) and (**2**).

[Fe^{II}(*H*CTPP*Me*)Br] (**1**): ^{1}H NMR (500 MHz, chloroform-d, 298 K): δ = 76.07 (s, 3H), 54.37 (s, 1H), 52.88 (s,

1H), 49.79 (s, 1H), 36.01 (s, 1H), 29.51 (s, 1H), 19.97 (s, 1H), 17.35 (s, 1H), 16.96 (s, 1H), 15.74 (s, 1H), 13.08 (s, 1H), 12.80 (s, 1H), 10.62 (s, 1H), 10.16 (s, 2H), 9.23 (s, 1H), 8.53 (s, 2H), 8.28 (s, 1H), 8.18 (s, 1H), 8.02 (s, 1H), 3.45 (s, 2H), 1.65 (s, 1H), -0.34 (s, 1H). UV-VIS (CH_2Cl_2) [λ_{max}, nm (log ε, $M^{-1}cm^{-1}$)]: 346 (4.49), 466 (5.02), 752 (4.32). HRMS (ESI-MS): Calcd. for $C_{45}H_{31}N_4FeBr$ $\{M\}^+$, 762.1081; Found: 762.1075.

[Fe^{II}(d_{20}-*H*CTPP*Me*)Br] (**1a**): ^{1}H NMR (500 MHz, chloroform-d, 298 K): δ = 74.88 (s, 3H), 53.36 (s, 1H), 51.91 (s, 1H), 48.65 (s, 1H), 35.61 (s, 1H), 29.18 (s, 1H), 16.71 (s, 1H), 15.63 (s, 1H), 10.61 (s, 1H).

[Fe^{II}(*H*CTPP*CD₃*)Br] (**1b**): ^{2}H NMR (76 MHz, CH_2Cl_2, 298 K): δ = 87.94 (vs. CD_2Cl_2).

[Fe^{II}(*Me*CTPP*Me*)Br] (**2**): ^{1}H NMR (400 MHz, chloroform-d, 298 K): δ = 58.58 (s, 3H), 56.08 (s, 1H), 54.54 (s, 1H), 50.06 (s, 1H), 45.99 (s, 2H), 34.34 (s, 1H), 27.49 (s, 1H), 21.53 (s, 1H), 19.40 (s, 1H), 17.94 (s, 1H), 16.38 (s, 1H), 13.29 (s, 2H), 10.02 (s, 2H), 8.48 (s, 2H), 8.28 (s, 1H), 8.21 (s, 1H), 7.95 (s, 2H), 7.66 (s, 1H), 6.17 (s, 1H), 5.36 (s, 2H), 4.47 (s, 2H), 1.96 (s, 1H) , -0.13 (s, 1H). UV-Vis (CH_2Cl_2) [λ_{max}, nm (log ε, $M^{-1}cm^{-1}$)]: 344 (4.46), 468(4.93), 756 (4.26). HRMS (ESI-MS): Calcd. for $C_{46}H_{33}N_4FeBr$ $\{M\}^+$, 776.1238; Found: 776.1234.

3. Synthesis of [Fe(CTPP*CH₂*)(NO)] (3). There are two methods to obtain [Fe(CTPP*CH₂*)NO] (**3**). Method A: in a N_2-filled dry box, [Fe^{II}(*HCTPPMe*)Br] (**1**) (20.8 mg, 0.0272 mmol) dissolved in 10 mL of anhydrous CH_2Cl_2 was added into 1.1 equiv of $NaNO_2$ (3.04×10^{-2} M in 1.0 mL MeOH), and the mixture was stirred at ambient temperature for 1.5 h. A completion of reaction was obtained when the *Soret* band was shifted from 466 nm, for starting [Fe^{II}(*HCTPPMe*)Br] (**1**), to 457 nm. Method B: in a N_2-filled dry box, [Fe^{II}(*HCTPPMe*)Br] (**1**) (11.1 mg, 0.0145 mmol) dissolved in 6 mL of anhydrous THF was added into 4.6 equiv of $NaNO_2$ (0.0667 mmol) and the mixture was stirred at ambient temperature for 24 h. Purification of **3**, from the crude mixtures prepared by both methods, was achieved by column chromatography under atmospheric conditions using a column filled with slurry basic alumina in CH_2Cl_2 (2 × 10 cm) and separated using gradient solvent from neat CH_2Cl_2 to CH_2Cl_2/acetone (*v*/*v*, 50:1). The major band as a brown solution was collected and dried under reduced pressure to obtain pure compound of [Fe(CTPP*CH₂*)(NO)] (**3**) (15.1 mg, 78% yield). Crystals suitable for X-ray diffraction analysis were obtained from vapor diffusion of *n*-hexane into a CH_2Cl_2 solution of **3**.

^{1}H NMR (400 MHz, chloroform-*d*, 298 K): δ = 10.14 (s, 1H), 8.72 (d, *J* = 4.8 Hz, 1H), 8.69 (d, *J* = 4.8 Hz, 1H), 8.58 (s, 1H), 8.50 (d, *J* = 6.8 Hz, 1H), 8.3–8.4 (m, 4H), 8.18 (d, *J* = 6.8 Hz, 1H), 8.14 (d, *J* = 7.0 Hz, 1H), 8.05 (d, *J* = 6.9 Hz, 1H), 8.00 (d, *J* = 7.4 Hz, 1H), 7.9–7.6 (m, 14H), -2.17 (s, 1H), -2.28 (s, 1H). UV-VIS (CH_2Cl_2) [λ_{max}, nm (log ε, $M^{-1}cm^{-1}$)]: 327 (4.35), 368 (4.38), 458 (4.62). HRMS (ESI-MS): Calcd. for $C_{45}H_{30}N_5FeO$ $\{M + H\}^+$, 712.1800; Found: 712.1805. FT-IR (KBr, cm^{-1}): 1704 (^{14}NO).

4. Synthesis of [Fe(CTPP*CH₂*)(^{15}NO)] (3a). Following the synthetic procedures for the preparation of **3**, [Fe^{II}(*HCTPPMe*)Br] (**1**) (20.3 mg, 0.0266 mmol) and $Na^{15}NO_2$ (6.1 mg, 0.087 mmol) were reacted in 10 mL mixed solvent of CH_2Cl_2/MeOH (10:1, *v*/*v*). After purification through basic alumina column chromatography, the final product [Fe(CTPP*CH₂*)(^{15}NO)] was obtained. FT-IR (KBr, cm^{-1}): 1672 ν(^{15}NO). ^{15}N NMR (50 MHz, chloroform-*d*, 298 K): δ = 93.21 ppm (vs. CH_3NO_2).

5. Synthesis of [Fe(d_{20}-CTPP*CH_2*)(NO)] (3b). Following the synthetic procedures for the preparation of [Fe(CTPP*CH_2*)NO] (**3**), [Fe^{II}(d_{20}-*HCTPPMe*)Br] (**1a**) (23.5 mg, 0.0300 mmol) and $NaNO_2$ (10.4 mg, 0.1507 mmol) were added to a mixed solvent of CH_2Cl_2/MeOH (12 mL, 12:1, *v*/*v*). After purification through basic alumina column chromatography, the final product [Fe(d_{20}-CTPP*CH_2*)(NO)] (**3b**) was obtained. ^{1}H NMR (400 MHz, chloroform-*d*, 298 K): δ = 10.14 (s, 1H), 8.71 (d, *J* = 4.8 Hz, 1H), 8.69 (d, *J* = 4.8 Hz, 1H), 8.3–8.4 (m, 4H), -2.17 (s, 1H), -2.28 (s, 1H).

6. Synthesis of [Fe(CTPP*CD_2*)(NO)] (3c). Following the synthetic procedures for the preparation of [Fe(CTPP*CH_2*)NO] (**3**), [Fe^{II}(*H*CTPP*CD_3*)Br] (**1b**) and $NaNO_2$ were reacted in a mixed solvent of CH_2Cl_2/MeOH (10 mL, 10:1, *v*/*v*). After purification through basic alumina column chromatography, the final product [Fe(CTPP*CD_2*)(NO)] (**3c**) was obtained. ^{1}H NMR (500 MHz, chloroform-*d*, 298 K): δ = 10.14 (s, 1H), 8.72 (d, *J* = 4.8 Hz, 1H), 8.69 (d, *J* = 4.8 Hz, 1H), 8.58 (s, 1H), 8.50 (d, *J* = 6.4 Hz, 1H), 8.3–8.4 (m, 4H), 8.18 (d, *J* = 6.7 Hz, 1H), 8.15 (d, *J* = 6.9 Hz, 1H), 8.05 (d, *J* = 7.1 Hz, 1H), 8.01 (d, *J* = 7.4 Hz, 1H), 7.9–7.6 (m, 14H). ^{2}H NMR (76 MHz, CH_2Cl_2 298 K): δ = -2.34 ppm (vs. CD_2Cl_2).

7. Time-dependent IR spectra of mixing [Fe^{II}(*H*CTPP*Me*)Br] (1) with [KNO_2][18-crown-6 ether]. In a N_2-filled dry box, a CH_2Cl_2 solution of [Fe^{II}(*HCTPPMe*)Br] (**1**) (0.5 mL, 6.42 × 10^{-3} M) in a syringe was injected into an sealed liquid cell with CaF_2 window. A glass-syringe filled with [KNO_2][18-crown-6 ether] solution in CH_2Cl_2 (1.00 × 10^{-2} M, 0.5 mL) was punched into the sealed liquid cell and brought out of the dry-box. Data recording process was executed immediately after [KNO_2][18-crown-6 ether] solution was injected into the cell and collected data for 1 hour.

8. Reaction of [Fe^{II}(*H*CTPP*Me*)Br] (1) with 1 equiv [PPN][NO_2] and hydroquinone. In a N_2-filled dry box, [Fe^{II}(*HCTPPMe*)Br] (**1**) (15.2 mg, 0.020 mmol) dissolved in 10 mL of anhydrous THF was added into 34.3 equiv of hydroquinone. The mixture was starred 0.5 h, and then added with 1.1 equiv of [PPN][NO_2] (12.4 mg in 0.5 mL ACN). The mixture was stirred at ambient temperature for 13 h, and the reaction was monitored by UV-Vis spectrophotometer. The *Soret* band was observed to shift from 467 nm to 440 nm after 2 h and then the absorbance of spectrum provided no further change until 13 h. The resulting UV-vis spectrum is consistent with Fe(CTPP*Me*)NO (**5**). Treating excess $AgBF_4$ into the reaction mixture afterward resulted a shift of *Soret* band from 440 to 474 nm. The resulting UV-vis spectrum is consistent with the [Fe(*H*CTPP*CH_2*)NO][BF_4] (**4**). Finally, we added several drops of TEA into the reaction mixture to observe the *Soret* band shifted from 474 nm to 458 nm. The pattern of the final UV-Vis spectrum is consistent with a Fe(CTPP*CH_2*)NO (**3**).

9. Reaction of [Fe^{II}(*H*CTPP*Me*)Br] (1) with 1 equiv [PPN][NO_2] in THF. In a N_2-filled dry box, [Fe^{II}(*HCTPPMe*)Br] (**1**) (8.1 mg, 0.011 mmol) dissolved in 0.8 mL of anhydrous THF was added with 1.4 equiv [PPN][NO_2] (13.4 mg in 0.2 mL ACN). The mixture was stirred at ambient temperature for 1 h and the reaction was monitored by using room-temperature ESI-Mass. In 15 minutes, the result of mass spectrum shows mass

peaks corresponding to [Fe(CTPP*Me*)(NO)] (**5**) ({M+H}$^+$: 713.1867), {[Fe^{III}(CTPP*Me*)]$_2$O} ({M + H}$^+$: 1381.3730), [Fe(CTPP*Me*)(NO$_2$)] ({M}$^+$: 728.1781), and [Fe(CTPP*Me*)(THF)] ({M + H}$^+$: 755.2437). In ^{1}H NMR spectrum ($CDCl_3$), the major proton resonances revealed one set from {FeNO}^{7} [Fe(d$_{20}$-CTPP*Me*)(NO)], one set from {FeNO}^{6} [Fe(d$_{20}$-CTPP*CH$_2$*)(NO)], and one set of broad proton signals around 14-15 ppm which is consistent with the anti-ferromagnetic complex, {[Fe(d$_{20}$-CTPP*Me*)]$_2$O} ({M + H}$^+$: 1421.6178). The ratio of [Fe(d$_{20}$-CTPP*Me*)(NO)] {FeNO}^{7} and {[Fe(d$_{20}$-CTPP*Me*)]$_2$O} are near 1:1 based on the integrated intensities of β−proton signals.

10. Reaction of [Fe^{II}(*Me*CTPP*Me*)Br] (2) with NaNO$_2$. In a N_2-filled dry box, [Fe^{II}(*MeCTPPMe*)Br] (**2**) (23.2 mg, 0.0298 mmol) dissolved in 15 mL of anhydrous THF was added into 3.30 equiv of $NaNO_2$. The reaction mixture was stirred at ambient temperature for 26 h. The reaction was continuously monitored by UV-Vis spectrophotometer, and no spectra change was observed within 26 h. Moreover, the ^{1}H NMR spectrum also shows the same β-proton signals as the starting [Fe^{II}(*MeCTPPMe*)Br] (**2**) after the reaction proceeded for 26 h.

11. Reaction of [Fe^{II}(*H*CTPP*Me*)Br] (1) with NaOMe than reacting with NaNO$_2$. In a N_2-filled dry box, [Fe^{II}(*HCTPPMe*)Br] (**1**) (20.0 mg, 0.0262 mmol) dissolved in 6 mL of anhydrous THF was added into 2.2 equiv of NaOMe (5.83×10^{-2} M in MeOH, 1.0 mL) and the mixture was stirred at ambient temperature for 0.5 h. A completion of reaction was obtained when the *Soret* band was shifted from 466 nm, for starting [Fe^{II}(*HCTPPMe*)Br] (**1**), to 470 nm. The solvent was removed under reduced pressure, and the solid was redissolved in small amount of CH_2Cl_2. The solution was filtered through a No. 2 paper filter to remove excess NaOMe and NaBr. The solvent was removed under reduced pressure again. The solid was redissolved in 10 mL of THF then added with 4.2 equiv $NaNO_2$. The mixture was starred at ambient temperature for 24 h, and the reaction was monitored by UV-Vis spectrophotometer. Throughout the 24 h, we did not detect any absorbance spectra with absorption bands related to NO complexes, such as [Fe(CTPP*CH$_2$*)NO] (**3**), [Fe(CTPP*Me*)NO] (**5**), and [Fe(*H*CTPP*CH$_2$*)(NO)]$^+$ (**4**) .

12. DFT calculations. The structures of [Fe(NCP*Me*)(HNO$_2$)] (S=0, **6a**; S=2, **6b**), [Fe(*H*NCP*Me*)(NO$_2$)] (S=0, **7a**; S=2, **7b**), [Fe(NCP*Me*)(ONOH)] (S=0, 8a; S=2, 8b), [Fe(*H*NCP*Me*)(ONO)] (S=0, **9a**; S=2, **9b**) are modified from crystal structure of [Fe^{II}(*H*CTPP*Me*)Br] (**1**). Moreover, the structures of [Fe(NCP*CH$_2$*)(NO)] {Fe(NO)}^{6} (**10**) and [Fe(NCP*Me*)(NO)] {FeNO}^{7} (**11**) were directly adopted from crystal structures of [Fe(CTPP*CH$_2$*)(NO)] (**3**) and [Fe(CTPP*Me*)(NO)] (**5**), respectively. The O-atom bonding nitrosyl iron NCP complexes of [Fe(NCP*CH$_2$*)(ON)] (**13**), and [Fe(NCP*Me*)(ON)] (**14**), and [Fe(NCP*Me*)(ON)]$^+$ (**15**) were modified from the optimized structure of **10**, **11**, and **12**,[1] respectively. All structures are fully optimized by using Gaussian 03 program[8] with BP86/TZVP method. The total energies of optimized structures are obtained with BP86/TZVP method for the determination of reaction energies. The N-confused porphyrin ligand is simplified with which the four phenyl groups are replaced by four hydrogen atoms and symbolled as NCP. The output data of all optimized

structures show no imaginary frequencies. Molecular orbitals were visualized by using Gauss View and molecular orbitals contributions were calculated by QMForge program.[9]

13. X-ray Single crystal structural determination. Diffraction measurements were carried out at 150(2) K on a Bruker SMART Apex CCD diffractometer equipped with graphite-monochromated Mo Kα radiation (λ = 0.71073 Å). The structures were solved by direct methods and refined using full-matrix least-squares methods against F^2 values using the SHELXTL4, 5 program packages. The positions of the hydrogen atoms were geometrically generated with a fixed distance and were assigned isotropic thermal parameters by the SHELXTL idealization methods. Refinement was carried out using anisotropic thermal parameters for all the non-hydrogen atoms. The absorption correction program SADABS was used for these three structures. Summary and experimental details for X-ray data collections are provided in Table S2. In the crystal structure of **2**, the dimethylated inverted pyrrole ring is disordered into two orientations with 0.75 and 0.25 site occupancy factors. The solvated CH_2Cl_2 has also been split into two sites with a 65% to 35% ratio. In the structure of **3**, mutual disorders on the outer pyrrolic nitrogen and the α-carbon of the inverted pyrrole ring were observed. A 50% site occupancy factor (*sof*) of nitrogen and a 50% *sof* of carbon were assigned to each atomic position using the *PART* command in SHELXTL program. The commands *EXYZ* and *EADP* were then applied to fix the coordinates and to average anisotropic displacement parameters, respectively.

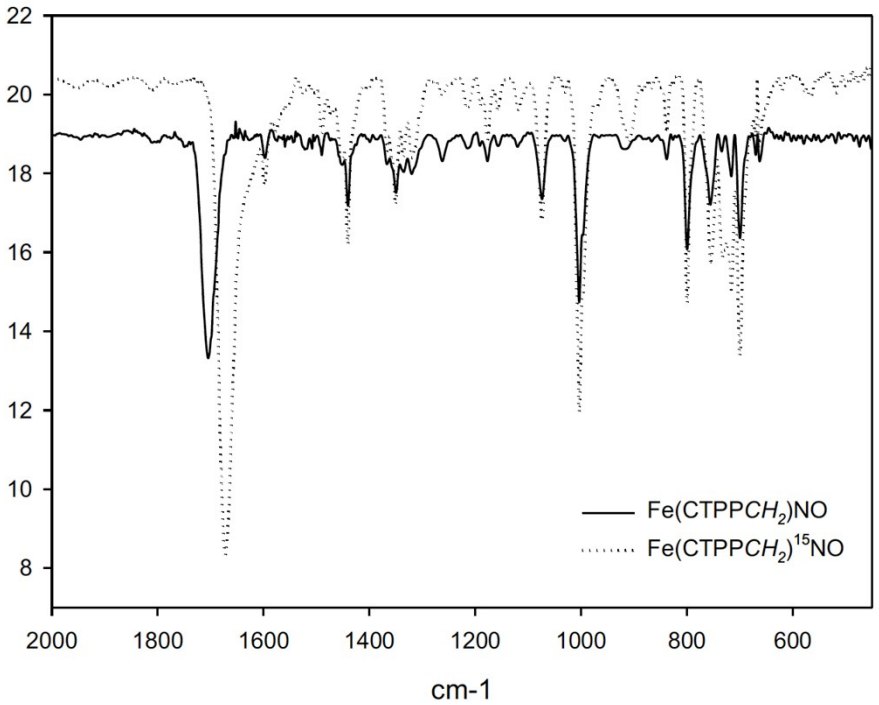

Figure S1. IR spectrum of Fe(CTPPCH_2)NO (**3**) and Fe(CTPPCH_2)^{15}NO (**3a**).

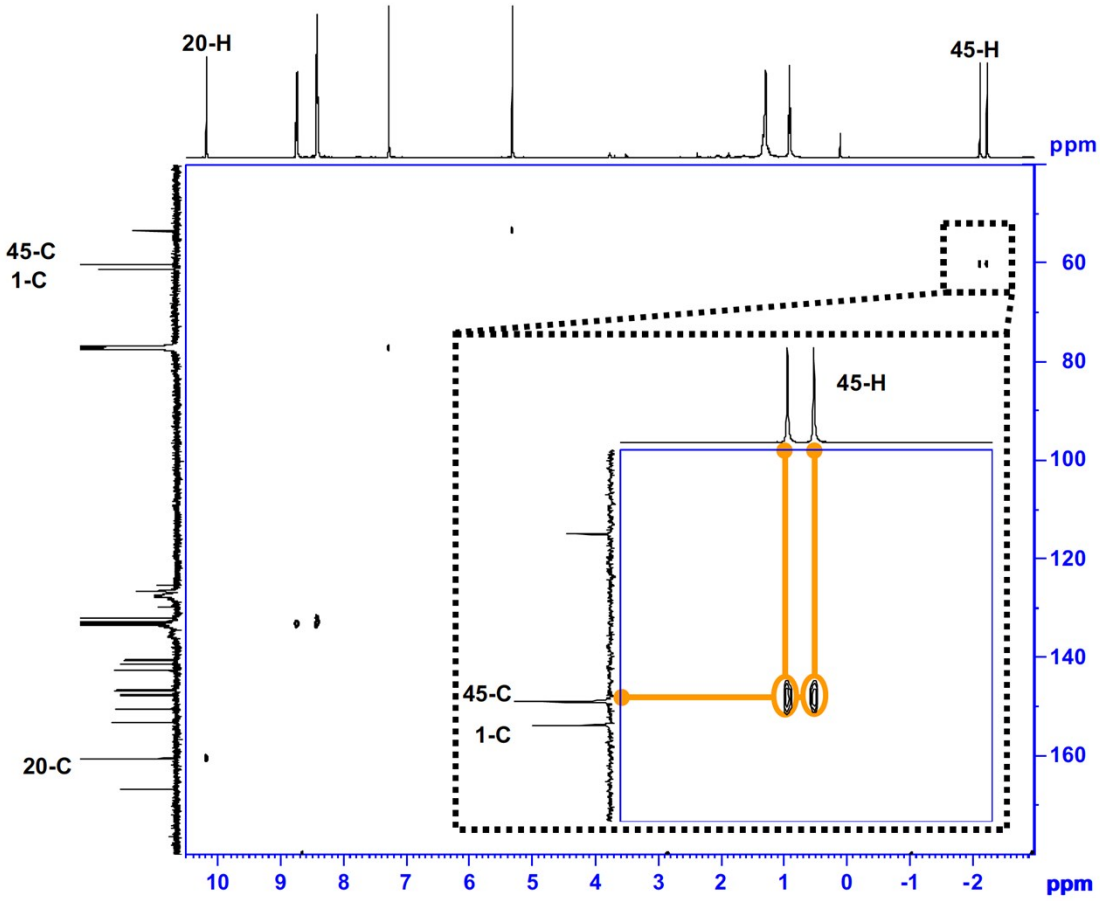

Figure S2. ^{1}H-^{13}C-HSQC of Fe(CTPPCH_2)NO (**3**) and inserted region of the methylene group.

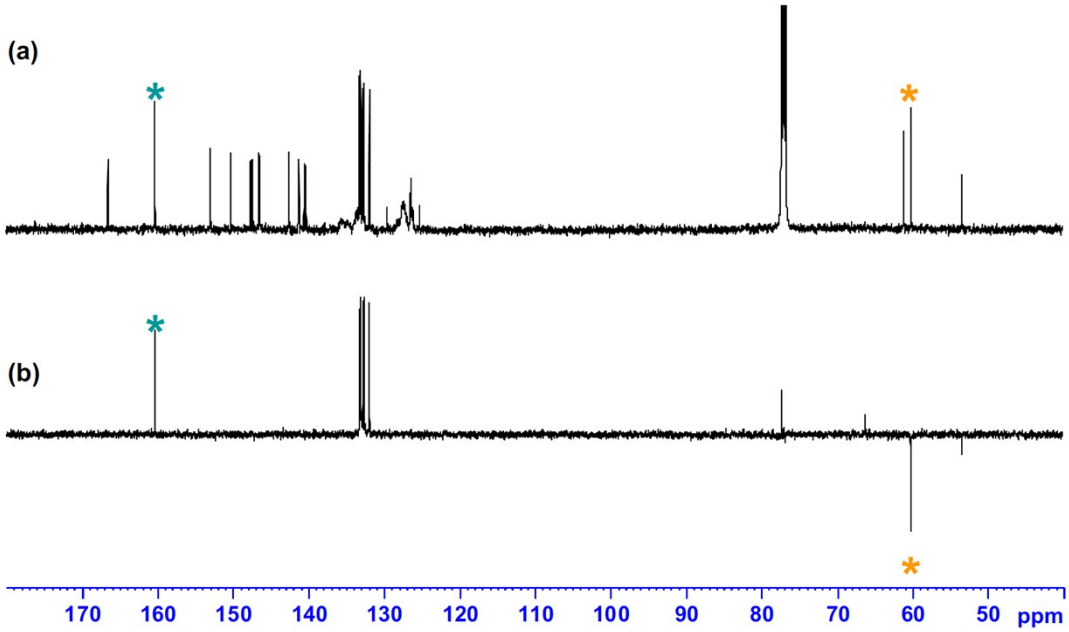

Figure S3. ^{13}C-NMR (upper) and DEP 135 (lower) of Fe(CTPPCH_2)NO (3, lower);

blue asterisk marks the carbon alongside the outer nitrogen and yellow asterisk marks the carbon of methylene group.

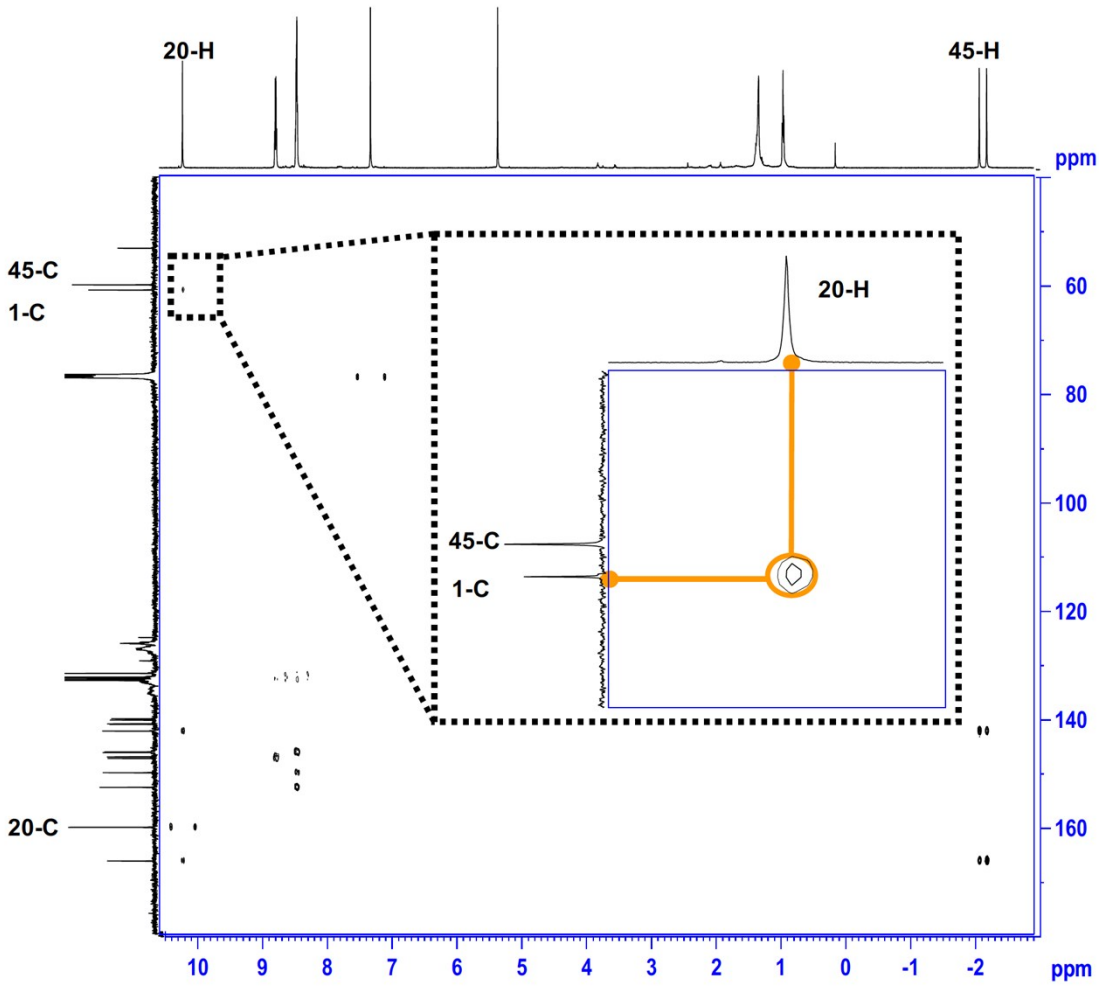

Figure S4. ^{1}H-^{13}C-HMBC of Fe(CTPPCH_2)NO (**3**) and inserted region of the inner-carbon.

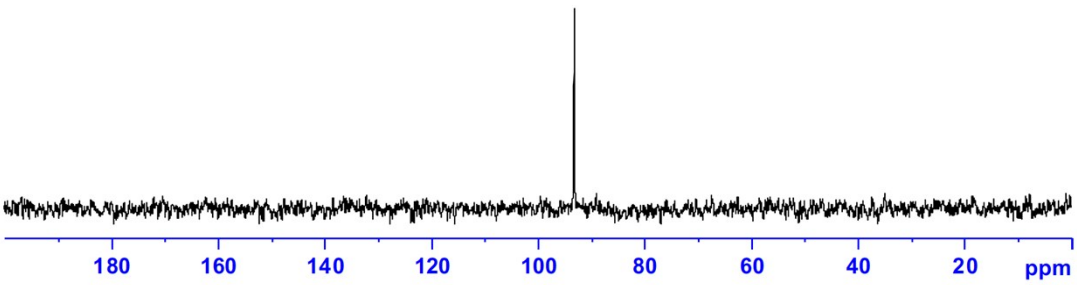

Figure S5. ^{15}N-NMR spectrum Fe(CTPPCH_2)^{15}NO (**3a**).

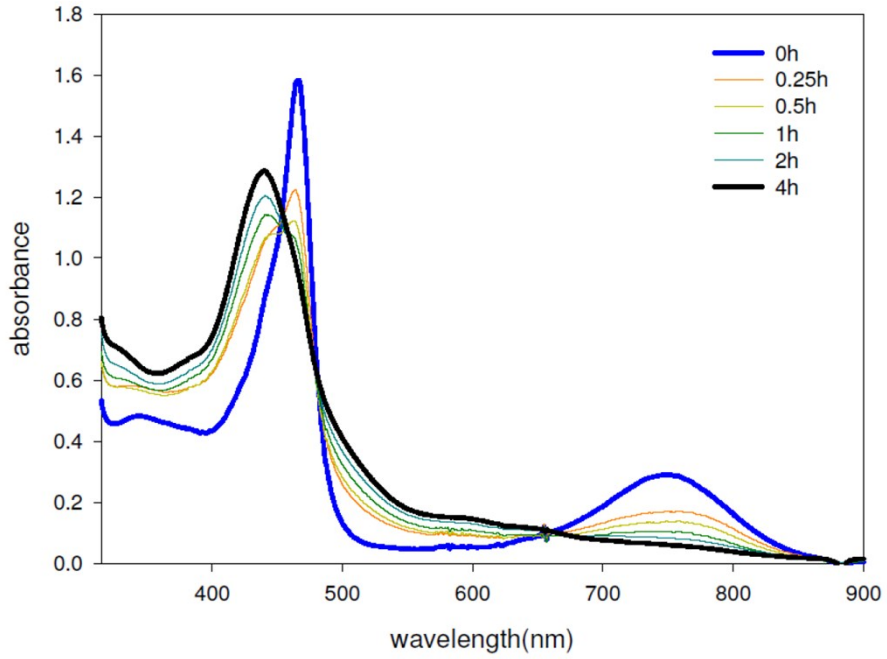

Figure S6. [Fe^{II}(*H*CTPP*Me*)Br] (**1**) reacted with 1 equiv. of $PPNNO_2$ and hydroquinone in 4 hours.

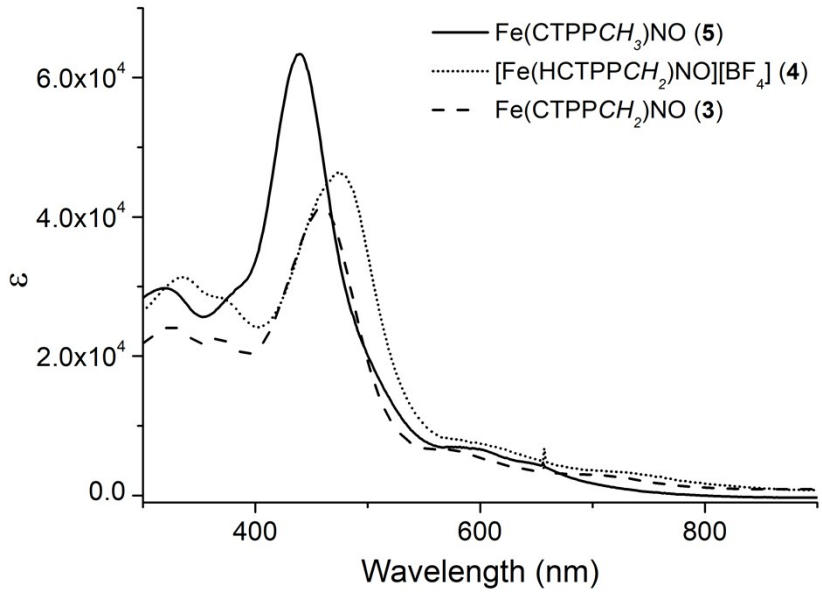

Figure S7. UV-Vis spectra of [Fe(CTPPCH_3)NO] (**5**, solid line), [Fe(*H*CTPPCH_2)NO][BF_4] (4, dotted line) and [Fe(CTPPCH_2)NO] (**3**, dashed line).

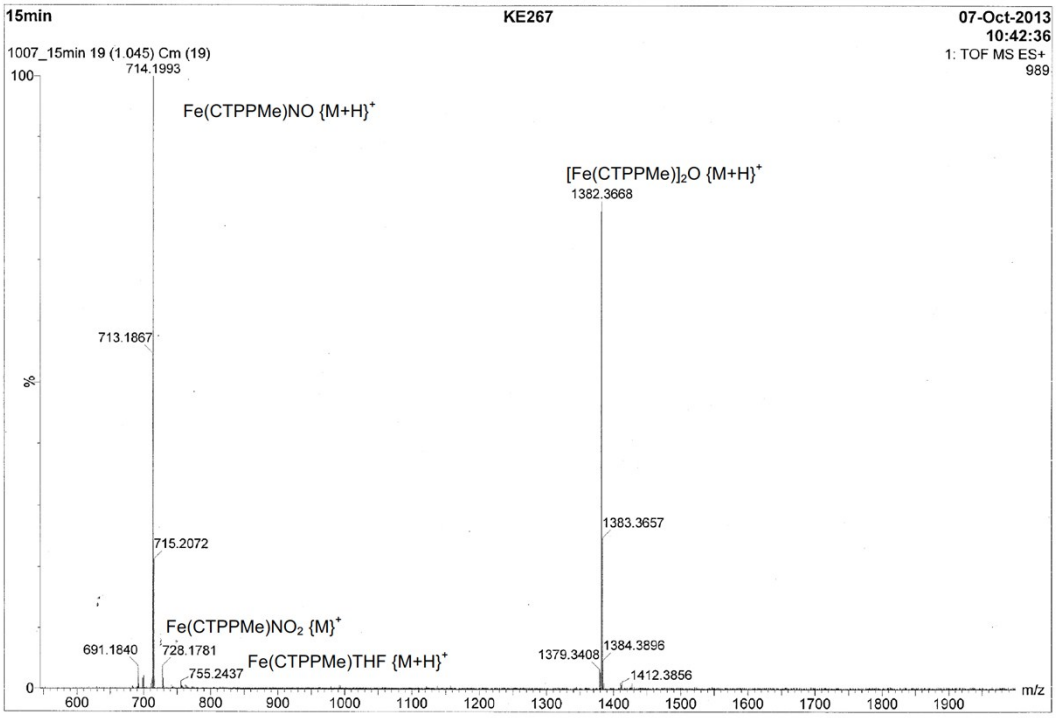

Figure S8. ESI-Mass spectrum of Reaction of [Fe^{II}(*HCTPPMe*)Br] (**1**) with 1 equiv [PPN][NO_2] in THF after 15 minutes

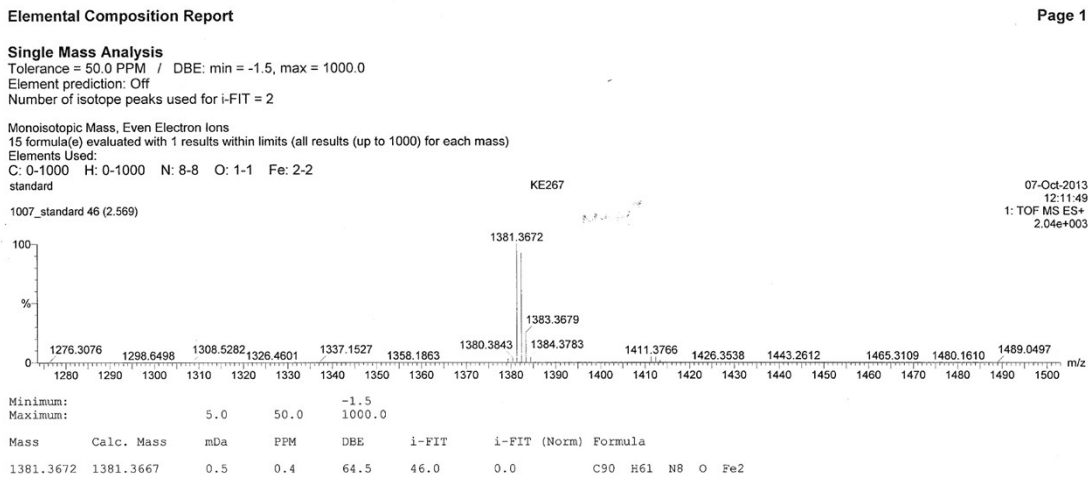

Elemental Composition Report **Page 1**

Single Mass Analysis
Tolerance = 50.0 PPM / DBE: min = -1.5, max = 1000.0
Element prediction: Off
Number of isotope peaks used for i-FIT = 2

Monoisotopic Mass, Even Electron Ions
15 formula(e) evaluated with 1 results within limits (all results (up to 1000) for each mass)
Elements Used:
C: 0-1000 H: 0-1000 N: 8-8 O: 1-1 Fe: 2-2

standard KE267 07-Oct-2013 12:11:49
1007_standard 46 (2.569) 1: TOF MS ES+ 2.04e+003

Minimum:				-1.5			
Maximum:		5.0	50.0	1000.0			
Mass	Calc. Mass	mDa	PPM	DBE	i-FIT	i-FIT (Norm)	Formula
1381.3672	1381.3667	0.5	0.4	64.5	46.0	0.0	C90 H61 N8 O Fe2

Figure S9. ESI-Mass spectrum analysis of [Fe^{III}(CTPP*Me*)]$_2$O $[M+H]^+$.

Elemental Composition Report **Page 1**

Single Mass Analysis
Tolerance = 50.0 PPM / DBE: min = -1.5, max = 1000.0
Element prediction: Off
Number of isotope peaks used for i-FIT = 2

Monoisotopic Mass, Even Electron Ions
8 formula(e) evaluated with 1 results within limits (all results (up to 1000) for each mass)
Elements Used:
C: 0-1000 H: 0-1000 N: 5-5 O: 2-2 Fe: 1-1

15min KE267 07-Oct-2013 10:42:36
1007_15min 19 (1.045) Cm (19) 1: TOF MS ES+ 3.68e+001

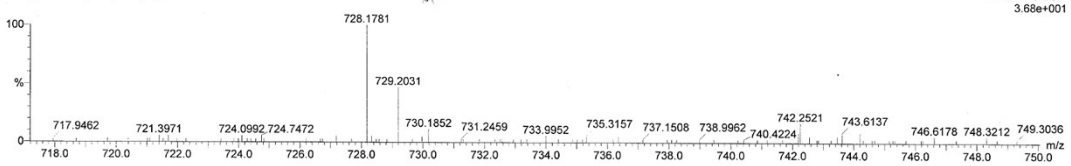

Minimum:				-1.5			
Maximum:		5.0	50.0	1000.0			
Mass	Calc. Mass	mDa	PPM	DBE	i-FIT	i-FIT (Norm)	Formula
728.1781	728.1749	3.2	4.4	33.5	32.0	0.0	C45 H30 N5 O2 Fe

Figure S10. ESI-Mass spectrum analysis of [Fe(CTPP*Me*)(NO_2)] $[M]^+$.

Elemental Composition Report **Page 1**

Single Mass Analysis
Tolerance = 50.0 PPM / DBE: min = -1.5, max = 1000.0
Element prediction: Off
Number of isotope peaks used for i-FIT = 2

Monoisotopic Mass, Even Electron Ions
9 formula(e) evaluated with 1 results within limits (all results (up to 1000) for each mass)
Elements Used:
C: 0-1000 H: 0-1000 N: 4-4 O: 1-1 Fe: 1-1

15min KE267 07-Oct-2013 10:42:36
1007_15min 12 (0.642) Cm (8:16) 1: TOF MS ES+ 5.06e+001

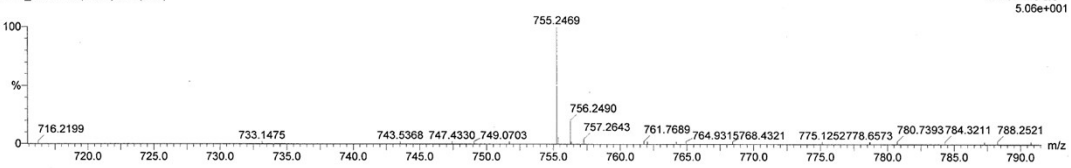

Minimum:				-1.5			
Maximum:		5.0	50.0	1000.0			
Mass	Calc. Mass	mDa	PPM	DBE	i-FIT	i-FIT (Norm)	Formula
755.2469	755.2473	-0.4	-0.5	32.5	28.1	0.0	C49 H39 N4 O Fe

Figure S11. ESI-Mass spectrum analysis of [Fe(CTPP*Me*)(THF)] $[M+H]^+$.

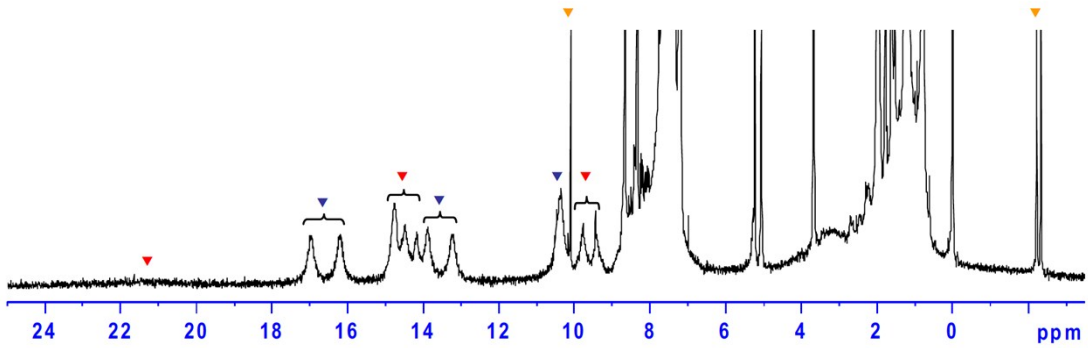

Figure S12. ^{1}H NMR spectrum of Reaction of [Fe^{II}(*HCTPPMe*)Br] (**1**) with 1 equiv. of [PPN][NO_2] in THF: Fe(CTPP*Me*)NO (**4**, blue marks), [Fe(CTPP*Me*)]$_2$O (red marks), and Fe(CTPPCH_2)NO (**3**, orange marks).

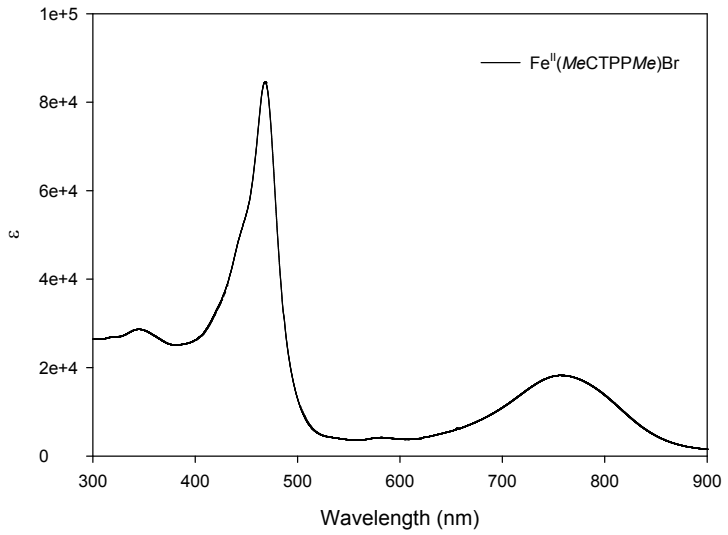

Figure S13. UV-Vis spectrum of Fe^{II}(*Me*CTPP*Me*)Br (**2**).

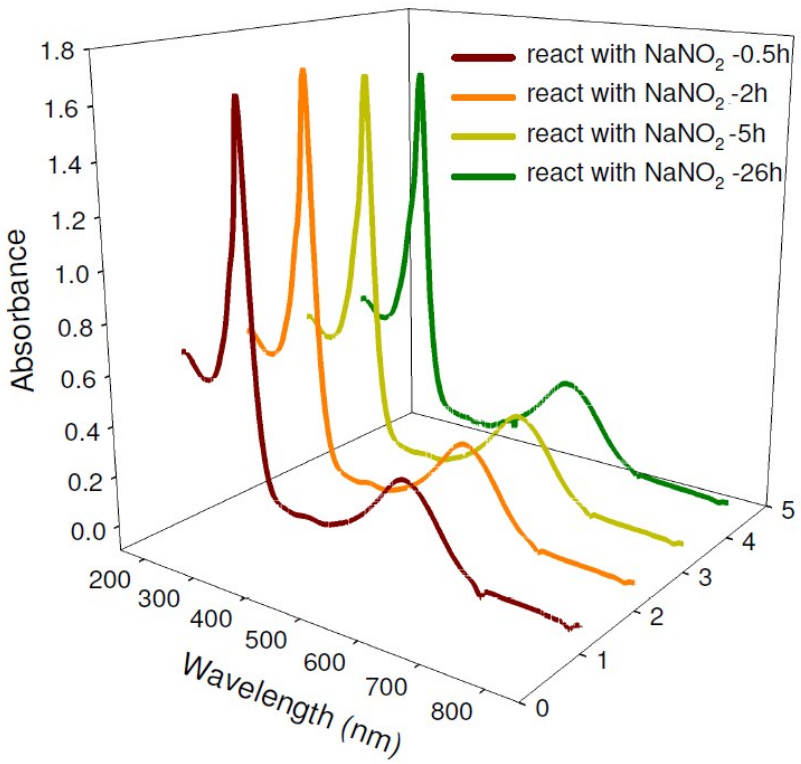

Figure S14. Fe^{II}(*Me*CTPP*Me*)Br (**2**) reacts with 1 equiv $NaNO_2$ for 24 hours.

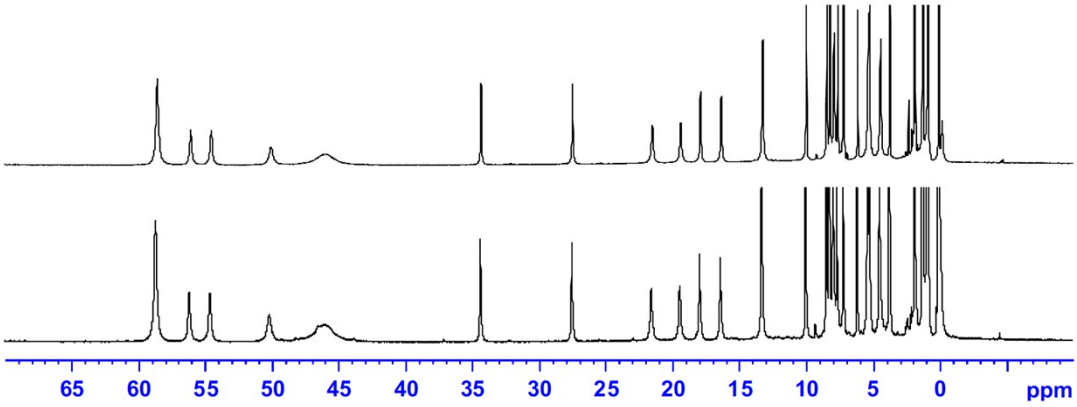

Figure S15. ^{1}H-NMR spectra of Fe^{II}(*Me*CTPP*Me*)Br (**2**, upper) and reaction after 24 hours (lower).

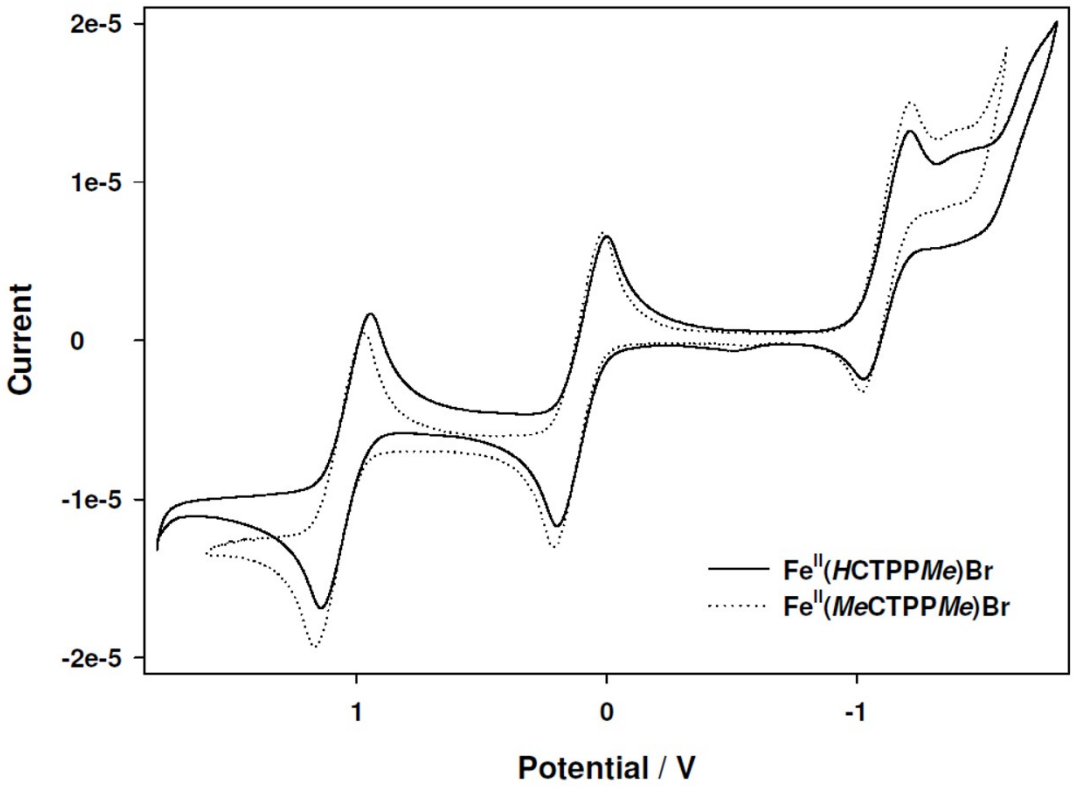

Figure S16. Cyclic voltammograms of Fe^{II}(*H*CTPP*Me*)Br (**1**) and Fe^{II}(*Me*CTPP*Me*)Br (**2**; vs $FeCp_2$).

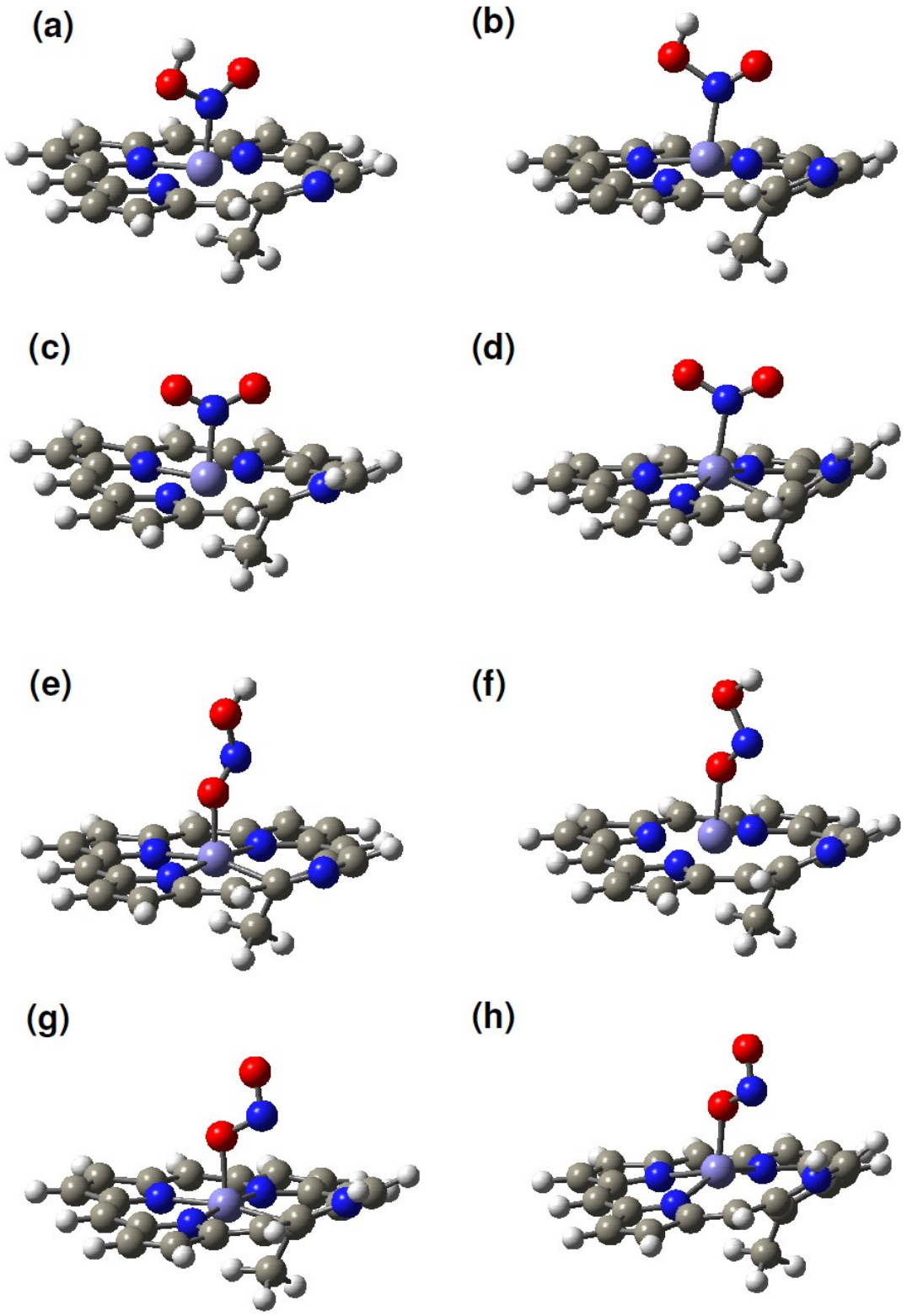
(a)
(b)
(c)
(d)
(e)
(f)
(g)
(h)

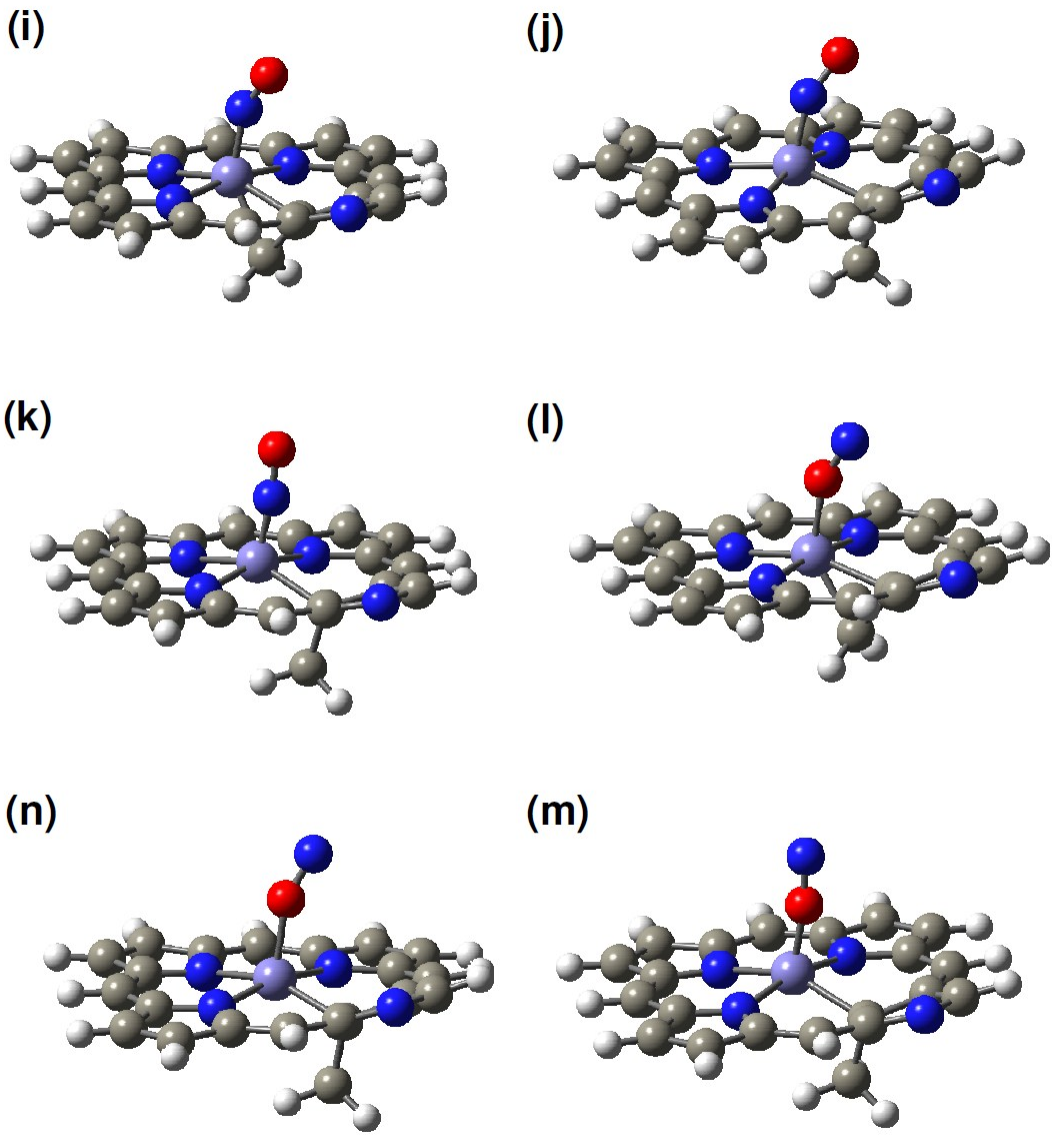

Figure S17. Optimized structures of **6a** (a), **6b** (b), **7a** (c), **7b** (d), **8a** (e), **8b** (f), **9a** (g), **9b** (h), **10** (i), **11** (j), **12** (k), **13** (l), **14** (n), and **15** (m).

Table S1. Optimized structures bond distances and Relative energies of Fe^{II}(NCP*Me*)(HNO_2) (**6a**).

Complex[a]	S	Fe-$N_{(NO2)}$	Fe-$O_{(NO2)}$	N-$O_{(NO2)}$	Fe-C	Fe-$C_{(CH3)}$	$\Delta E_{(kcal/mple)}$
Fe(CTPP*CH*$_2$)NO **(3)**[c]	0	**1.700**	–	1.176	2.089	1.975	–
Fe(CTPP*Me*)NO **(4)**[b, c]	1/2	**1.678**	–	1.177	2.072	2.647	–
Fe^{II}(NCP*Me*)(HNO_2) **(6a)**	0	**1.781**	–	1.474 $_{(HO-N)}$, 1.215 $_{(N=O)}$	2.067	2.251	0
Fe^{II}(NCP*Me*)(HNO_2) **(6b)**	2	**1.999**	–	1.455 $_{(HO-N)}$, 1.210 $_{(N=O)}$	2.233	2.641	+21.81
Fe^{II}(*H*NCP*Me*)(NO_2) **(7a)**	0	**1.917**	–	1.241, 1.246	2.115	2.237	+ 4.85
Fe^{II}(*H*NCP*Me*)(NO_2) **(7b)**	2	**2.084**	–	1.249	2.320	2.654	+18.85
Fe^{II}(NCP*Me*)(ONOH) **(8a)**	0	–	**1.854**	1.426 $_{(HO-N)}$, 1.239 $_{(N=O)}$	2.069	2.185	+18.05
Fe^{II}(NCP*Me*)(ONOH) **(8b)**	2	–	**1.997**	1.438 $_{(HO-N)}$,1.226$_{(N=O)}$	2.222	2.587	+27.97
Fe^{II}(*H*NCP*Me*)(ONO) **(9a)**	0	–	**1.902**	1.363 $_{(O-N)}$, 1.218$_{(N=O)}$	2.084	2.173	+15.84
Fe^{II}(*H*NCP*Me*)(ONO) **(9b)**	2	–	**1.939**	1.364 $_{(O-N)}$, 1.211$_{(N=O)}$	2.296	2.678	+18.31
Fe(NCP*CH*$_2$)NO **(10)**	0	**1.694**	–	1.176	2.100	1.975	**-28.82**
Fe(NCP*Me*)NO **(11)**[b]	1/2	**1.693**	–	1.184	2.075	2.715	+38.31
[Fe(NCP*Me*)NO]$^+$ **(12)**[b]	0	**1.618**	–	1.160	2.082	2.663	+145.00
Fe(NCP*CH*$_2$)ON **(13)**	0	–	**1.795**	**1.172**	2.102	1.952	+5.97
Fe(NCP*Me*)ON **(14)**	1/2	–	**1.871**	**1.186**	2.083	2.699	+71.85
[Fe(NCP*Me*)ON]$^+$ **(15)**	0	–	**1.698**	**1.162**	2.086	2.650	+186.90
NO_2^-	0	–	–	1.279	–	–	–
HNO_2	0	–	–	1.444 $_{(HO-N)}$, 1.187 $_{(N=O)}$	–	–	–

[a]All optimized structures and single point energies obtain with BP86/TZVP; [b]ref 1; [c]crystal structure.

Table S2. Crystal Data and Structure Refinement for **Fe^{II}(*Me*CTPP*Me)*Br (2)** and

Fe(CTPP*CH₂*)NO (3).

	Fe^{II}(*Me*CTPP*Me)*Br (2)	**Fe(CTPP*CH₂*)NO (3)**
formula	$C_{46.5}H_{34}BrClFeN_4$	$C_{46}H_{31}Cl_2FeN_5O$
formula weight	819.98	796.51
crystal system	Triclinic	Triclinic
space group	*P-1*	*P-1*
a, Å	12.4481(4)	10.4707(5)
b, Å	12.8921(4)	13.0591(6)
c, Å	13.1225(5)	14.8946(7)
α, deg	89.986(2)	89.716(2)
β, deg	80.134(2)	75.015(2)
γ, deg	67.664(2)	68.874(2)
V, Å^3	1914.25(11)	1826.35(15)
Z value	2	2
ρ_{calc}, g/cm^3	1.423	1.448
μ, mm^{-1}	1.547	0.605
F_{000}	838	820
T, K	150(2)	150(2)
	$-14 \leqq h \leqq 14$	$-12 \leqq h \leqq 12$
hkl ranges	$-13 \leqq k \leqq 15$	$-15 \leqq k \leqq 8$
	$-15 \leqq l \leqq 15$	$-17 \leqq l \leqq 16$
GOF	1.018	1.029
R_1, wR_2 (I>2σ(I))	0.0569, 0.1552	0.0534, 0.1152

$R_1 = \Sigma \| F_o | - | F_c \| / \Sigma | F_o |$; $wR_2 = [\Sigma w(F_o^2 - F_c^2)^2 / \Sigma w(F_o^2)^2]^{1/2}$; $w = 1/\sigma^2(|F_o|)$

1. Ching, W.-M.; Hung, C.-H., *Chem. Commun.* **2012,** *48*, 4989-4991.
2. Schmidt, I.; Chmielewski, P. J., *Inorg. Chem.* **2003,** *42*, 5579-5593.
3. Chmielewski, P. J.; Latos-Grażyński, L.; Głowiak, T., *J. Am. Chem. Soc.* **1996,** *118*, 5690-5701.
4. Geier, G. R.; Haynes, D. M.; Lindsey, J. S., *Org. Lett.* **1999,** *1*, 1455-1458.
5. Rachlewicz, K.; Wang, S.-L.; Ko, J.-L.; Hung, C.-H.; Latos-Grażyński, L., *J. Am. Chem. Soc.* **2004,** *126*, 4420-4431.
6. Chen, W.-C.; Hung, C.-H., *Inorg. Chem.* **2001,** *40*, 5070-5071.
7. Rachlewicz, K.; Gorzelańczyk, D.; Latos-Grażyński, L., *Inorg. Chem.* **2006,** *45*, 9742-9747.
8. Frisch, M. J. e. a., *Gaussain 03*, Gaussian, Inc., Wallingford CT, 2004.
9. Pellegrino, J.; Bari, S. E.; Bikiel, D. E.; Doctorovich, F., *J Am Chem Soc* **2010,** *132*, 989-95.